math xmlns="http://www.w3.org/1998/Math/MathML">mrow>msub>mi>J/mi>mi>eff/mi>/msub>mo>=/mo>mfrac>mn>3/mn>mn>2/mn>/mfrac>/mrow>/math> metallic phase and unconventional superconductivity in math xmlns="http://www.w3.org/1998/Math/MathML">mrow>msub>mi>GaTa/mi>mn>4/mn>/msub>msub>mi>Se/mi>mn>8/mn>/msub>/mrow>/math>

Min Yong Jeong, Seo Hyoung Chang, Hyeong Jun Lee, Jae-Hoon Sim, Kyeong Jun Lee, Etienne Janod, Laurent Cario, Ayman Said, Wenli Bi, Philipp Werner, Ara Go, Jungho Kim, and Myung Joon Han

Phys. Rev. B **103**, L081112 — Published 24 February 2021

DOI: 10.1103/PhysRevB.103.L081112

Novel $J_{\rm eff}$=3/2 Metallic Phase and Unconventional Superconductivity in $GaTa_4Se_8$

Min Yong Jeong,[1] Seo Hyoung Chang,[2] Hyeong Jun Lee,[3] Jae-Hoon Sim,[1,4] Kyeong Jun Lee,[2] Etienne Janod,[5] Laurent Cario,[5] Ayman Said,[6] Wenli Bi,[7] Philipp Werner,[8] Ara Go,[3,9,*] Jungho Kim,[6,†] and Myung Joon Han[1,‡]

[1]*Department of Physics, Korea Advanced Institute of Science and Technology, Daejeon 34141, Korea*
[2]*Department of Physics, Chung-Ang University, Seoul 06974, South Korea*
[3]*Center for Theoretical Physics of Complex Systems, Institute for Basic Science (IBS), Daejeon 34126, Korea*
[4]*CPHT, CNRS, Ecole Polytechnique, Institut Polytechnique de Paris, F-91128 Palaiseau, France*
[5]*Institut des Matériaux Jean Rouxel (IMN), Université de Nantes, CNRS, 2 Rue de la Houssinière, BP32229, 44322 Nantes cedex 3, France*
[6]*Advanced Photon Source, Argonne National Laboratory, Argonne, IL 60439, USA*
[7]*Department of Physics, University of Alabama at Birmingham, Birmingham, AL, 35294, USA*
[8]*Department of Physics, University of Fribourg, 1700 Fribourg, Switzerland*
[9]*Department of Physics, Chonnam National University, Gwangju 61186, Korea*

(Dated: February 8, 2021)

By means of density functional theory plus dynamical mean-field theory (DFT+DMFT) calculations and resonant inelastic x-ray scattering (RIXS) experiments, we investigate the high-pressure phases of the spin-orbit-coupled $J_{\rm eff} = 3/2$ insulator $GaTa_4Se_8$. Its metallic phase, derived from the Mott state by applying pressure, is found to carry $J_{\rm eff} = 3/2$ moments. The characteristic excitation peak in the RIXS spectrum maintains its destructive quantum interference of $J_{\rm eff}$ at the Ta L_2-edge up to 10.4 GPa. Our exact diagonalization based DFT+DMFT calculations including spin-orbit coupling also reveal that the $J_{\rm eff} = 3/2$ character can be clearly identified under high pressure. These results establish the intriguing nature of the correlated metallic magnetic phase, which represents the first confirmed example of $J_{\rm eff}$=3/2 moments residing in a metal. They also indicate that the pressure-induced superconductivity is likely unconventional and influenced by these $J_{\rm eff} = 3/2$ moments. Based on a self-energy analysis, we furthermore propose the possibility of doping-induced superconductivity related to a spin-freezing crossover.

Introduction – Identifying and characterizing the phases and phase transitions of materials is a central theme of condensed matter physics. The discovery of a new type of phase often requires theoretical analyses of its essential nature, as well as clarifications of the relationship to other known phases and the possible transitions into nearby phases. As a well-known example, unconventional metal states in cuprate phase diagram hold many mysteries [1–4]. Being clearly different from a Fermi liquid, these anomalous metallic phases can be a precursor or competitor of unconventional superconductivity [5–7].

The lacunar spinel GaM_4X_8 (M=V, Nb, Ta, Mo; X=S, Se, Te) is a fascinating class of materials which exhibits multiferroic, skyrmion, and resistive switching phenomena [8–14]. $GaTa_4Se_8$, in particular, has been highlighted as an interesting example that undergoes a paramagnetic Mott insulator to metal transition (IMT) under pressure [15–18]. Furthermore, recent studies elucidated the significant effect of spin-orbit coupling (SOC) and showed that its ground state carries spin-orbit entangled (so-called) $J_{\rm eff}$=3/2 moments [19–21], which is the first confirmed example of this kind. Considering the observed IMT followed by a superconducting transition as a function of pressure, the identification of the $J_{\rm eff}$=3/2 Mott phase at ambient conditions immediately generates a series of important questions: If the metallic phase is a conventional Fermi liquid, it is a more or less trivial case, and the superconductivity observed at higher pressures is also likely of the conventional type. On the other hand, if it is a correlated metal which still hosts $J_{\rm eff} = 3/2$ moments, it can be regarded as a new type of metallic phase, and the observed superconductivity is more likely to be unconventional.

In this Letter, we try to elucidate the nature of the pressure-induced metallic phase which emerges out of the Mott insulator without doping. By means of resonant inelastic x-ray scattering (RIXS) experiments and density functional theory plus dynamical mean-field theory (DFT+DMFT) calculations, we investigate its detailed electronic and magnetic properties. We find that the characteristic L_3 peak is clearly observed even in the metallic regime while the forbidden L_2 peak is absent. This observation together with the simulation results clearly identifies the novel metallic state with $J_{\rm eff} = 3/2$ magnetic moments. We discuss its implications regarding the superconductivity at higher pressure. Finally, we explore another intriguing possibility in this material. Our self-energy analysis shows that electron doping can induce a spin-freezing crossover, a phenomenon which has been previously linked to unconventional superconductivity [22]. These results will hopefully stimulate experimental efforts to clarify the properties of this material under chemical or other types of doping.

Electronic structure and insulator-metal-superconductor transition – $GaTa_4Se_8$ is composed of well-separated $GaSe_4$ and Ta_4Se_4 molecular clusters

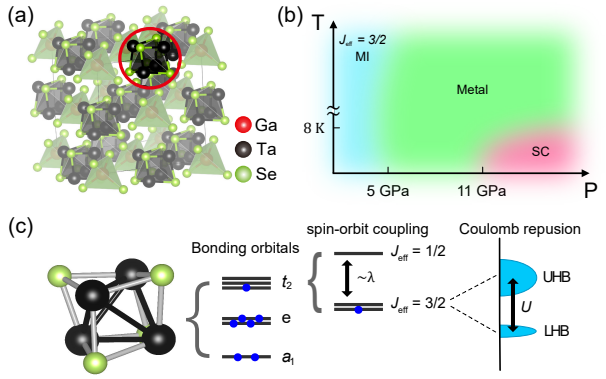

FIG. 1. (a) Crystal structure of $GaTa_4Se_8$. Red, black and green spheres represent the Ga, Ta and Se atoms, respectively. (b) A schematic pressure-temperature phase diagram of $GaTa_4Se_8$. The cyan, green and red colored region represents the $J_{\rm eff} = 3/2$ Mott insulating, metallic and superconducting phases, respectively. It should be noted that the phase boundary lines have not yet been well identified due to the lack of experimental information. (c) Schematic electronic structure near E_F which is dominated by molecular orbital states of the higher-lying t_2 and lower-lying e and a_1 type. The t_2 levels are further split into $J_{\rm eff} = 1/2$ and 3/2 by SOC. At ambient pressure, the Mott gap is stabilized by the on-site Coulomb interaction U.

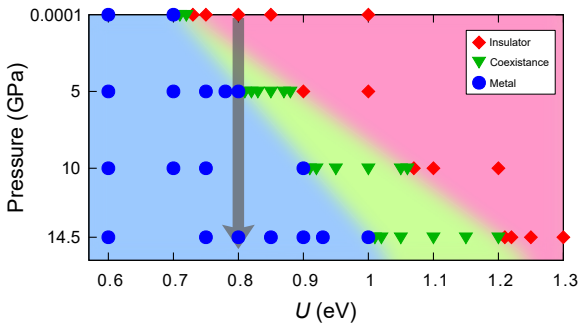

FIG. 2. Calculated phase diagram for $GaTa_4Se_8$ as a function of U and pressure within DFT+DMFT+SOC (at zero temperature). Blue circles, red diamonds and green triangles represent the calculated points corresponding to the metallic, insulating, and coexistence phase, respectively. The realistic value of $U \approx 0.8$ eV is depicted by a gray arrow.

as shown in Fig. 1(a). The Fermi level (E_F) is dominated by t_2 molecular orbitals which are derived from Ta-t_{2g} atomic orbitals [14–18, 20, 21, 23, 24]. On top of the spin-orbit splitted molecular $J_{\rm eff} = 3/2$ quartet and $J_{\rm eff} = 1/2$ doublet, the on-site Coulomb interaction (U) induces a Mott gap in the quater-filled $J_{\rm eff} = 3/2$ bands; see Fig. 1(c) [20, 21]. This spin-orbit entangled molecular $J_{\rm eff} = 3/2$ Mott phase was first predicted by DFT+SOC+U calculations [20] and then confirmed by RIXS experiments [21]. Here the 'on-site' Coulomb repulsion U represents the interaction within molecular t_2 orbitals rather than atomic Ta orbitals [16, 18, 23].

Largely unexplored are the IMT and the metal-to-superconductor transition, both of which are induced by applying pressure (without doping; see Fig. 1(b)) [15–18]. The pressure-dependent crystal structure data [16] indicate that the Mott IMT is caused by the increased hopping integrals between the Ta_4Se_4 molecular units. This bandwidth controlled IMT was studied based on the three-orbital Hubbard model within DMFT-QMC (quantum Monte Carlo) [18]. However, the effect of SOC has not been taken into account and therefore the $J_{\rm eff} = 3/2$ state could not be realized.

DFT+DMFT phase diagram: The effect of SOC – With this motivation, we first performed DFT+DMFT calculations with SOC (See Supplemental Materials for computation details [25]). The calculated phase diagram is presented in Fig. 2. The red and blue colored regions represent the insulating and metallic phases, respectively. We note that at $U > 0.7$ eV, pressure can always induce the transition and that the critical value of U_c is gradually increased as pressure increases.

By including SOC, the calculated phase diagram shows a good quantitative agreement with the experiments. Considering the neglected frequency dependence of U in the DMFT procedure, we expect that the realistic effective interaction strength is slightly larger than the constrained random phase approximation (cRPA) value of $U_{\rm cRPA} = 0.7$ eV; $U \approx 0.7$-0.9 eV [26]. With $U = 0.8$ eV, the IMT occurs at $P \approx 5$ GPa as shown in Fig. 2. This is in good agreement with previous experimental data reporting a critical pressure P_c of 5-7 GPa [17, 18]. It is important to note that, in the previous DMFT calculations (without SOC), the critical U_c of 1.2 eV [18] is significantly larger than our value. Also, if we follow Ref. 18 and identify the calculated coexistence region with the hysteresis region observed at intermediate pressure in the resistivity measurement [18], our results are in even better agreement with the experiment. Hence, without the effect of SOC, the experimental phase boundary cannot be well reproduced and the $J_{\rm eff} = 3/2$ moments are not formed.

Metallic $J_{\rm eff}$=3/2 states: RIXS experiment – The direct evidence of the novel $J_{\rm eff} = 3/2$ Mott phase at ambient pressure came from RIXS [21]. As an element-specific photon-in and photon-out measurement using dipole transitions between Ta $5d$ and $2p_{3/2}$ (L_3) or $2p_{1/2}$ (L_2), RIXS was able to detect and compare the excitation spectra at both edges. The compelling evidence for $J_{\rm eff} = 3/2$ was the presence and the absence of a ~1.3 eV peak at L_3 and L_2, respectively, which is directly based on the quantum mechanical selection rules [21]. Here we adopt the same approach to probe $J_{\rm eff} = 3/2$ moments in the metallic regime and perform the pressure-dependent RIXS measurements (See Supplemental Materials for experimental details [25]).

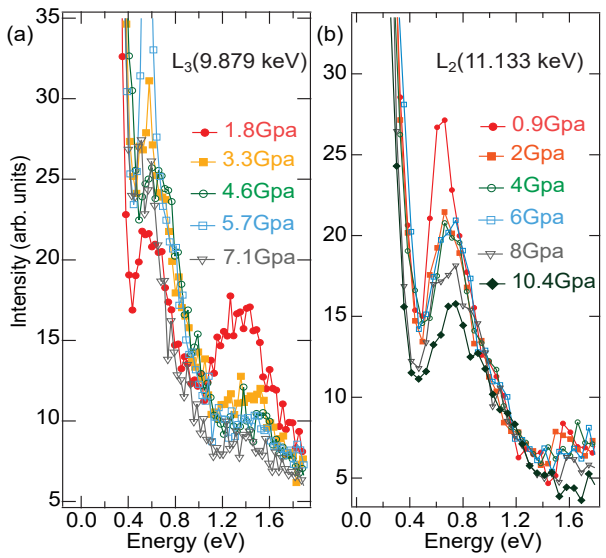

FIG. 3. (a, b) Pressure-dependent RIXS data at the (a) L_3 and (b) L_2 edge. The different symbols and colors represent different pressure values.

Figure 3(a) shows the RIXS spectra at the L_3-edge under pressure. The positive sign in the energy represents energy loss. Strong low energy intensities for all high-pressures are mostly attributed to an extrinsic scattering from high-pressure environments such as the Be gasket and the diamond anvils, and those intensity tails largely affect the spectral features below 0.4 eV [27]. The insulating phase (1.8 GPa) spectrum shows two broad features around 0.7 eV and 1.3 eV. At higher pressures, low energy high-pressure environment scattering intensities become stronger, leading to seemingly larger intensities around 0.7 eV, because the gasket and the diamond anvil become closer to the sample at high pressure. The sharp peak around 0.7 eV seen at 3.3 and 5.7 GPa comes from high-pressure environments. On the other hand, the 1.3 eV peak feature is marginally affected by the tail of the extrinsic scattering and free from any sharp high-pressure environment scattering peak. The 1.3 eV peak originates from the orbital excitation in between the occupied e and a_1 state and the unoccupied $J_{\rm eff} = 1/2$ state [21]. The ambient pressure RIXS measurement showed that the 1.3 eV peak intensity is largely modulated with the crystal momentum transfer and the sample angle [21]. The 1.3 eV peak intensity is weak in the sample orientation used for the spectra in Fig. 3(a). It is important to note that the 1.3 eV broad feature is, although weak, visible up to the metallic phase (5.7 and 7.1 GPa) and its energy position and width more or less stays the same. For further analysis, see Supplemental Materials [25].

Figure 3(b) presents our main experimental RIXS spectra at the L_2-edge under high pressure. In this high-pressure sample, the extrinsic scatterings from high-pressure environments happened to be weaker compared to the case of the L_3-edge measurement, and therefore, we resolve orbital excitations above 0.4 eV without high-pressure environment contamination: the low energy extrinsic scattering intensities are similar for all high pressures and no sharp high-pressure environment scattering peak is seen. The 0.7 eV peak at the L_2-edge was assigned, in the previous work, to excitations from the occupied e and a_1 to the unoccupied $J_{\rm eff} = 3/2$ states [21]. Upon entering the coexistence regime ($P \sim 2$ GPa; orange), the peak becomes broadened with its intensity reduced. Up to 6 GPa, the peak width and energy are insensitive to the pressure. In the metallic phase ($P =$ 8 and 10.4 GPa; gray and black), the peak width is further broadened. A more itinerant $J_{\rm eff} = 3/2$ state may contribute to the peak broadening in the high-pressure metallic phase by affecting the local coherent RIXS process. Consistent with the ambient pressure RIXS study, the insulating phase spectrum (P =0.9 GPa; red) shows that the 1.3 eV orbital excitation seen at the L_3-edge is totally suppressed at the L_2-edge due to the destructive quantum interference of the $J_{\rm eff}$ state. Importantly, the spectral intensity profile in the 1.3 eV excitation region is insensitive to the applied higher pressure up to 10.4 GPa, confirming that the $J_{\rm eff}$ state persists in the high-pressure metallic phase.

Arguably, this is the first verification of a metallic phase hosting $J_{\rm eff}$=3/2 moments. In the most studied case of a metallic phase derived from a magnetic Mott insulator (*e.g.,* cuprates), the magnetic order is quickly destroyed by doping. Recalling that the doping of a Mott insulator with S=1/2 moments can lead to different intriguing phases such as the pseudogap and strange metal phase, or superconductivity, our finding of a metallic $J_{\rm eff}$=3/2 phase deserves further investigations regarding its nature and relation to superconductivity, which are discussed further in the below.

Metallic $J_{\rm eff}$=3/2 states: DFT+DMFT calculation – In order to further elucidate the characteristics of this novel metallic phase, we performed many-body electronic structure calculations. The DFT+DMFT spectral functions are presented in Fig. 4. At ambient pressure (Fig. 4(a)), the Mott gap is clearly observed and the upper/lower Hubbard bands are of $J_{\rm eff} = 3/2$ character. The gap size of 0.4–0.6 eV is in good agreement with optical conductivity data [17]. At $P \geq 5$ GPa (Fig. 4(b) and (c)), the gap is closed and the system becomes metallic, with a characteristic quasiparticle peak forming at E_F. It should be noted that this correlated metallic feature of the spectral function cannot be captured by the static approximation. See Supplemental Materials for more details [25].

An important observation is that the center of mass position of the higher-lying $J_{\rm eff} = 1/2$ states does not move but remains basically unchanged, even though the spectral weight of the $J_{\rm eff} = 1/2$ states is significantly redistributed by varying pressure. The arrows in Fig. 4 con-

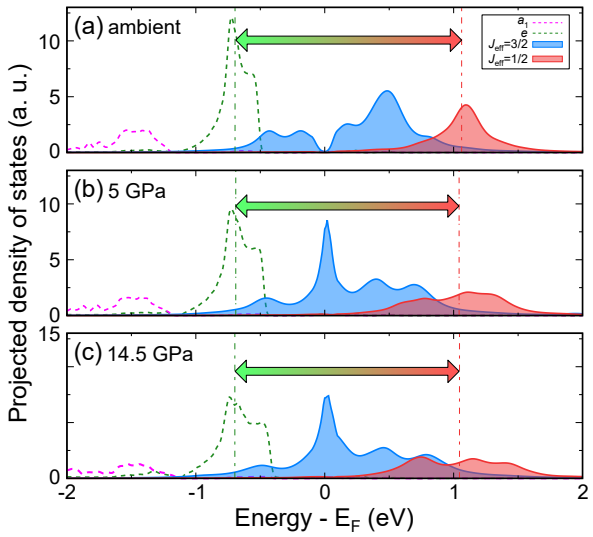

FIG. 4. (a-c) Calculated spectral functions at (a) $P = 0$, (b) 5 and (c) 14.5 GPa. The filled blue and red solid lines represent the molecular $J_{\rm eff} = 3/2$ and $J_{\rm eff} = 1/2$ states, respectively. The dashed magenta and green lines present the a_1 and e states, respectively. The arrows connect the center of mass positions of the $J_{\rm eff} = 1/2$ and e states.

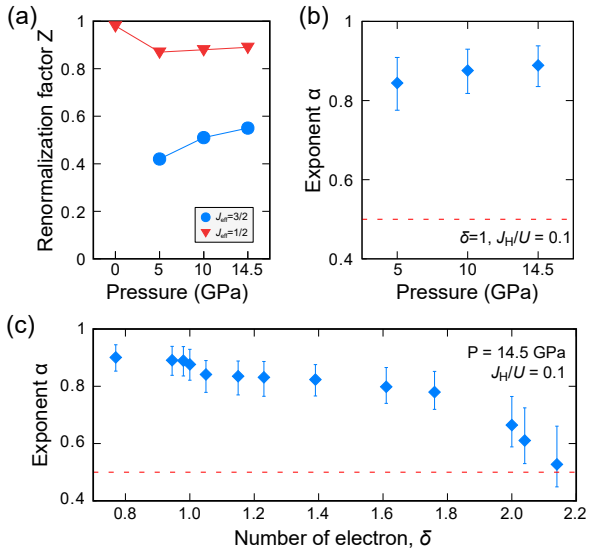

FIG. 5. (a) Calculated renormalization factor Z as a function of pressure. Blue circles (red triangles) show the Z of the $J_{\rm eff} = 3/2$ ($J_{\rm eff} = 1/2$) bands. (b, c) The calculated exponent α as a function of (b) pressure and (c) electron number. The horizontal red dashed lines show $\alpha = 0.5$, namely, the exponent value typically associated with a spin-freezing crossover[37]. The density of electrons $\delta = 1$ corresponds to pristine $GaTa_4Se_8$. For the exponent fitting, $J_{\rm H}/U = 0.1$ is used with U=0.8 eV.

nect the center of mass positions of the e (dashed green lines) and $J_{\rm eff} = 1/2$ (red solid lines) states, and their length is almost independent of pressure. This is particularly important because the $J_{\rm eff} = 1/2 \rightarrow e$ transition is mainly responsible for the L_3 peak at +1.3 eV observed in our RIXS measurement (see Fig. 3(a)) [21]. Therefore, our DMFT calculation (including SOC) strongly supports our interpretation of the RIXS spectra; namely, the 1.3 eV peak should persist even for the reshaped spectral functions in the metallic phase [28]. An additional supporting analysis can be found in Ref. 25.

Another noticeable feature is that the low energy states (forming the 'coherent peak') in the metallic phase are still of $J_{\rm eff} = 3/2$ character, see Fig. 4(b) and (c). This may have important implications for superconductivity. Recalling the cuprate phase diagram, for example, the Mott insulating state with antiferromagnetic spin order is destroyed by doping and followed by a pseudogap phase before superconductivity appears at low temperature. At higher temperatures, the pseudogap state is followed by the so-called strange metal, whose characteristics are clearly distinct from a Fermi liquid. In studies of the two-dimensional Hubbard model, it has recently been shown that these non-Fermi liquid phases host long-lived composite spin-1 moments [29, 30]. In this regard, identifying the $J_{\rm eff} = 3/2$ nature of the metallic phase of $GaTa_4Se_8$ may be relevant for understanding the superconductivity observed at higher pressures.

To gain further insights into the character of this novel metallic phase, we perform a self-energy analysis. The renormalization factor Z, defined as $\lim_{\omega\rightarrow 0}[1 - \frac{\partial}{\partial\omega}{\rm Re}\Sigma(\omega)]^{-1}$, shows that this pressure-induced phase exhibits sizable electronic correlations, which is reminiscent of the pseudogap or strange metal region of cuprates. Figure 5(a) shows that $Z_{J_{\rm eff}=3/2}$ (blue circles) is well below 1.0 while it gradually increases as a function of pressure. This is in contrast to the result for the $J_{\rm eff} = 1/2$ bands (red triangles) whose Z value remains close to unity in a wide pressure range.

For cuprates, the relation between the pseudogap phase and superconductivity has long been a central topic of research [2–4, 6, 30, 31]. Also, recent theoretical studies on half Heusler alloys suggest possible superconductivity arising from a $J = 3/2$ band structure [32–36]. Here it is presumed that the observed superconducitivity at higher pressure is unconventional since it emerges out of a novel correlated metallic phase with $J_{\rm eff} = 3/2$ in proximity to a Mott insulator.

Doping and spin-freezing superconductivity – Finally, we explore and suggest another intruiging possibility in this material. Recent multi-band DMFT calculations showed that unconventional superconductivity can arise from a so-called spin-freezing crossover [22, 29, 37–39] although this mechanism still requires experimental confirmation. In order to check this scenario in the case of $GaTa_4Se_8$, we perform a self-energy analysis. Following Ref. 37, $-{\rm Im}\Sigma(i\omega_n)$ is fitted in the low-energy region with the function $\Gamma + C \cdot (\omega_n)^{\alpha}$, where Γ, C, and α are con-

stants, and ω_n denotes Matsubara frequencies. A Fermi liquid is characterized by $\mathrm{Im}\Sigma(i\omega_n) \sim \omega_n$; namely, $\Gamma \approx 0$ and $\alpha \approx 1.0$ [40–42]. In the moment freezing regime, on the other hand, the self-energy behavior clearly deviates from this linear dependence [40, 41], with $\alpha < 1$.

The calculated α is presented as a function of pressure in Fig. 5(b) with $J_{\mathrm{H}}/U = 0.1$ where we considered the range of $0.1 \lesssim \omega_n/D \lesssim 0.3$ (D is the half bandwidth) for the fitting. The error bars reflect the deviations caused by varying the fitting range [25]. In the metallic regime of $P \geq 5$ GPa, α increases as a function of pressure, which is reasonable in the sense that the system becomes more metallic or closer to a Fermi liquid. Note that α is well above the value $\alpha = 1/2$ typically associated with the spin freezing crossover, which may indicate that the known pressure-induced superconductivity is not primarily driven by local moment fluctuations. In fact, in this $\delta = 1$ system with one electron per t_2 molecular orbital, the role of the Hund's interaction J_{H} likely becomes less pronounced [40, 42], although a J-freezing crossover has been reported in model calculations [38] with SOC.

On the other hand, we clearly find that introducing extra charges induces a moment freezing crossover in $GaTa_4Se_8$. Figure 5(c) shows the calculated exponent α as a function of δ (the electron number per t_2 molecular orbital). While Γ remains quite small, α is gradually decreased as δ increases. In particular, at around $\delta \approx$ 1.8–2.0, a substantial drop is observed, indicative of a spin freezing crossover [37]. This result is also consistent with the previous model study on a Bethe lattice [38]. Thus, an unconventional type of superconductivity, possibly distinct from the pressure-induced superconductivity at zero doping, can be expected to occur under electron doping.

In order to introduce extra electrons into $GaTa_4X_8$, the chemical substitution of Ge for Ga can be considered, and has been already reported for $(Ga/Ge)V_4S_8$ [43]. Doping alkali- or alkaline-earth metals is another possible way to achieve a spin-freezing crossover. As a 'deficient' spinel structure (*i.e.,* AB_2X_4 spinel with half-deficient A sites), lacunar spinels can likely host additional alkali- or alkaline-earth metals. While a spin freezing crossover has been previously suggested for multi-band transition-metal perovskite oxides [40], it is awaiting experimental confirmation. Here we note that this prediction is based on the idealized model density of states (DOS) of the Bethe lattice. While the spin freezing crossover appears in between two extreme limits of spin states, this idealized DOS shape can easily be broken up in a real material. Then the system is driven to more stable ordered phases such as antiferromagnetic, ferromagnetic and/or orbital ordered phases, rather than the less stable superconducting phase. This may be the reason why in many multi-band perovskite oxides no superconductivity has been identified. In this regard, $GaTa_4X_8$ can be an interesting playground because its DOS shape is better retained due to its molecular nature. Namely, even under pressure, the lattice degree of freedom is less active and the electronic degeneracy is well maintained. In fact, the main change of the lattice structure as a function of pressure is the reduction of the inter-cluster distance, while the molecular units are largely unchanged [16]. Thus $GaTa_4Se_8$ can be an ideal platform to explore this type of unconventional superconductivity.

Summary – We demonstrated that the metallic phase of $GaTa_4Se_8$ carries J_{eff}=3/2 moments and exhibits sizable correlations. Our RIXS spectra clearly show that the characteristic orbital excitation features are well maintained under pressure, which is consistent with the results of our DFT+DMFT calculations. The pressure-induced phase can therefore be regarded as a novel type of correlated metallic phase. Simultaneously, this conclusion suggests that the superconductivity appearing at higher pressure is likely unconventional. Furthermore, our self-energy analysis indicates that an unconventional type of superconductivity may emerge from a J-freezing crossover under electron doping. Our results highlight a new material phase that has not been observed before, and provides an exciting new playground for exploring unconventional types of superconducting instabilities.

M.Y.J. and S.H.C. contributed equally to this work. The use of the Advanced Photon Source at the Argonne National Laboratory was supported by the U.S. DOE under Contract No. DE-AC02-06CH11357. M.Y.J., J.-H.S and M.J.H were supported by Basic Science Research Program (2018R1A2B2005204), and Creative Materials Discovery Program through NRF (2018M3D1A1058754) funded by the Ministry of Science and ICT (MSIT) of Korea, and the KAIST Grand Challenge 30 Project (KC30) in 2019 funded by the MSIT of Korea and KAIST.

* arago@jnu.ac.kr
† jhkim@anl.gov
‡ mj.han@kaist.ac.kr

[1] E. Fradkin, S. A. Kivelson, and J. M. Tranquada, Rev. Mod. Phys. **87**, 457 (2015).
[2] M. R. Norman, D. Pines, and C. Kallin, Advances in Physics **54**, 715 (2005).
[3] P. A. Lee, N. Nagaosa, and X.-G. Wen, Rev. Mod. Phys. **78**, 17 (2006).
[4] B. Keimer and J. E. Moore, Nature Phys **13**, 1045 (2017).
[5] D. N. Basov, R. D. Averitt, D. van der Marel, M. Dressel, and K. Haule, Rev. Mod. Phys. **83**, 471 (2011).
[6] D. J. Scalapino, Rev. Mod. Phys. **84**, 1383 (2012).
[7] A. Kapitulnik, S. A. Kivelson, and B. Spivak, Rev. Mod. Phys. **91**, 011002 (2019).
[8] I. Kézsmárki, S. Bordács, P. Milde, E. Neuber, L. M. Eng, J. S. White, H. M. Ronnow, C. D. Dewhurst, M. Mochizuki, K. Yanai, H. Nakamura, D. Ehlers, V. Tsurkan, and A. Loidl, Nature Materials **14**, 1116 (2015).
[9] E. Ruff, S. Widmann, P. Lunkenheimer, V. Tsurkan,

S. Bordács, I. Kézsmárki, and A. Loidl, Science Advances **1**, e1500916 (2015).
[10] Y. Fujima, N. Abe, Y. Tokunaga, and T. Arima, Phys. Rev. B **95**, 180410 (2017).
[11] E. Ruff, A. Butykai, K. Geirhos, S. Widmann, V. Tsurkan, E. Stefanet, I. Kézsmárki, A. Loidl, and P. Lunkenheimer, Phys. Rev. B **96**, 165119 (2017).
[12] K. Geirhos, S. Krohns, H. Nakamura, T. Waki, Y. Tabata, I. Kézsmárki, and P. Lunkenheimer, Phys. Rev. B **98**, 224306 (2018).
[13] V. Guiot, E. Janod, B. Corraze, and L. Cario, Chem. Mater. **23**, 2611 (2011).
[14] V. Dubost, T. Cren, C. Vaju, L. Cario, B. Corraze, E. Janod, F. Debontridder, and D. Roditchev, Nano Lett. **13**, 3648 (2013).
[15] M. M. Abd-Elmeguid, B. Ni, D. I. Khomskii, R. Pocha, D. Johrendt, X. Wang, and K. Syassen, Physical Review Letters **93** (2004), 10.1103/PhysRevLett.93.126403.
[16] R. Pocha, D. Johrendt, B. Ni, and M. M. Abd-Elmeguid, Journal of the American Chemical Society **127**, 8732 (2005).
[17] V. Ta Phuoc, C. Vaju, B. Corraze, R. Sopracase, A. Perucchi, C. Marini, P. Postorino, M. Chligui, S. Lupi, E. Janod, and L. Cario, Physical Review Letters **110** (2013), 10.1103/PhysRevLett.110.037401.
[18] A. Camjayi, C. Acha, R. Weht, M. G. Rodríguez, B. Corraze, E. Janod, L. Cario, and M. Rozenberg, Physical Review Letters **113** (2014), 10.1103/PhysRevLett.113.086404.
[19] B. J. Kim, H. Jin, S. J. Moon, J.-Y. Kim, B.-G. Park, C. S. Leem, J. Yu, T. W. Noh, C. Kim, S.-J. Oh, J.-H. Park, V. Durairaj, G. Cao, and E. Rotenberg, Physical Review Letters **101** (2008), 10.1103/PhysRevLett.101.076402.
[20] H.-S. Kim, J. Im, M. J. Han, and H. Jin, Nature Communications **5** (2014), 10.1038/ncomms4988.
[21] M. Y. Jeong, S. H. Chang, B. H. Kim, J.-H. Sim, A. Said, D. Casa, T. Gog, E. Janod, L. Cario, S. Yunoki, M. J. Han, and J. Kim, Nature Communications **8**, 782 (2017).
[22] S. Hoshino and P. Werner, Phys. Rev. Lett. **115**, 247001 (2015).
[23] R. Pocha, D. Johrendt, and R. Pöttgen, Chem. Mater. **12**, 2882 (2000).
[24] A. Camjayi, R. Weht, and M. J. Rozenberg, EPL **100**, 57004 (2012).
[25] See Supplemental Materials [url] for the computational details, experimental details and complementary data, which includes Refs. [44–62].
[26] M. Casula, P. Werner, L. Vaugier, F. Aryasetiawan, T. Miyake, A. J. Millis, and S. Biermann, Phys. Rev. Lett. **109**, 126408 (2012).
[27] J. Kim, High Pressure Res. **36**, 391 (2016).
[28] This weight transfer might be responsible for the reduction of L_3 RIXS peak height as a function of pressure (see Fig. 3(b)) which needs further clarification.
[29] P. Werner, S. Hoshino, and H. Shinaoka, Phys. Rev. B **94**, 245134 (2016).
[30] P. Werner, X. Chen, and E. Gull, Phys. Rev. Research **2**, 023037 (2020).
[31] E. Gull, O. Parcollet, and A. J. Millis, Phys. Rev. Lett. **110**, 216405 (2013).
[32] P. Brydon, L. Wang, M. Weinert, and D. Agterberg, Phys. Rev. Lett. **116**, 177001 (2016).
[33] C. Timm, A. P. Schnyder, D. F. Agterberg, and P. M. R. Brydon, Phys. Rev. B **96**, 094526 (2017).
[34] H. Kim, K. Wang, Y. Nakajima, R. Hu, S. Ziemak, P. Syers, L. Wang, H. Hodovanets, J. D. Denlinger, P. M. R. Brydon, D. F. Agterberg, M. A. Tanatar, R. Prozorov, and J. Paglione, Science Advances **4**, eaao4513 (2018).
[35] J. W. Venderbos, L. Savary, J. Ruhman, P. A. Lee, and L. Fu, Phys. Rev. X **8**, 011029 (2018).
[36] G. Sim, A. Mishra, M. J. Park, Y. B. Kim, G. Y. Cho, and S. Lee, Phys. Rev. B **100**, 064509 (2019).
[37] P. Werner, E. Gull, M. Troyer, and A. J. Millis, Phys. Rev. Lett. **101**, 166405 (2008).
[38] A. J. Kim, H. O. Jeschke, P. Werner, and R. ValentÃ, Phys. Rev. Lett. **118**, 086401 (2017).
[39] P. Werner and S. Hoshino, Phys. Rev. B **101**, 041104 (2020).
[40] A. Georges, L. d. Medici, and J. Mravlje, Annu. Rev. Condens. Matter Phys. **4**, 137 (2013).
[41] A. Kowalski, A. Hausoel, M. Wallerberger, P. Gunacker, and G. Sangiovanni, Phys. Rev. B **99**, 155112 (2019).
[42] K. Stadler, G. Kotliar, A. Weichselbaum, and J. von Delft, Annals of Physics **405**, 365 (2019).
[43] E. Janod, E. Dorolti, B. Corraze, V. Guiot, S. Salmon, V. Pop, F. Christien, and L. Cario, Chem. Mater. **27**, 4398 (2015).
[44] T. Ozaki, Phys. Rev. B **67**, 155108 (2003).
[45] I. Leonov, A. I. Poteryaev, V. I. Anisimov, and D. Vollhardt, Phys. Rev. Lett. **106**, 106405 (2011).
[46] K. Haule and T. Birol, Phys. Rev. Lett. **115**, 256402 (2015).
[47] I. Leonov, S. L. Skornyakov, V. I. Anisimov, and D. Vollhardt, Phys. Rev. Lett. **115**, 106402 (2015).
[48] S. L. Skornyakov, V. I. Anisimov, D. Vollhardt, and I. Leonov, Phys. Rev. B **96**, 035137 (2017).
[49] N. Marzari and D. Vanderbilt, Phys. Rev. B **56**, 12847 (1997).
[50] I. Souza, N. Marzari, and D. Vanderbilt, Physical Review B **65**, 035109 (2001).
[51] F. Aryasetiawan, K. Karlsson, O. Jepsen, and U. Schönbergerr, Phys. Rev. B **74**, 125106 (2006).
[52] E. Şaşıoğlu, C. Friedrich, and S. Blügel, Phys. Rev. B **83**, 121101 (2011).
[53] D. Sénéchal, Phys. Rev. B **81**, 235125 (2010).
[54] A. Go and A. J. Millis, Phys. Rev. Lett. **114**, 016402 (2015).
[55] A. Go and A. J. Millis, Phys. Rev. B **96**, 085139 (2017).
[56] E. Fertitta and G. H. Booth, Phys. Rev. B **98**, 235132 (2018).
[57] N.-O. Linden, M. Zingl, C. Hubig, O. Parcollet, and U. Schollwöck, Phys. Rev. B **101**, 041101 (2020).
[58] Y. Shvyd'ko, J. Hill, C. Burns, D. Coburn, B. Brajuskovic, D. Casa, K. Goetze, T. Gog, R. Khachatryan, J.-H. Kim, C. Kodituwakku, M. Ramanathan, T. Roberts, A. Said, H. Sinn, D. Shu, S. Stoupin, M. Upton, M. Wieczorek, and H. Yavas, J. Electron. Spectrosc. Relat. Phenom. **188**, 140 (2013).
[59] M. Rossi, C. Henriquet, J. Jacobs, C. Donnerer, S. Boseggia, A. Al-Zein, R. Fumagalli, Y. Yao, J. G. Vale, E. C. Hunter, R. S. Perry, I. Kantor, G. Garbarino, W. Crichton, G. Monaco, D. F. McMorrow, M. Krisch, and M. M. Sala, J. Synchrotron Rad. **26**, 1725 (2019).
[60] G. Kotliar, S. Y. Savrasov, K. Haule, V. S. Oudovenko, O. Parcollet, and C. A. Marianetti, Rev. Mod. Phys. **78**,

865 (2006).
[61] H.-S. Kim, K. Haule, and D. Vanderbilt, Phys. Rev. B **102**, 081105 (2020).
[62] Z. P. Yin, K. Haule, and G. Kotliar, Phys. Rev. B **86**, 195141 (2012).